https://doi.org/10.5194/hess-2021-455
Preprint. Discussion started: 7 October 2021

Hydrology and Earth System Sciences
Discussions
Open Access
EGU

Continuous Monitoring of a Soil Aquifer Treatment System's Physico-Chemical Conditions to Optimize Operational Performance

Tuvia Turkeltaub[1], Alex Furman[2], Ron Mannheim[2], Noam Weisbrod[1]

[1]Department of Environmental Hydrology and Microbiology, Zuckerberg Institute for Water Research, The Jacob Blaustein Institutes for Desert Research, Ben-Gurion University of the Negev, Sede Boqer Campus, Midreshet Ben-Gurion, 84990 Israel.

[2]Technion – Israel Institute of Technology, Civil and Environmental Engineering, Haifa 32000, Israel

Correspondence to: Tuvia Turkeltaub (tuviat@bgu.ac.il)

Highlights

- *Long wetting stages reduce soil percolation capabilities during winter.*
- *E_h and gaseous O_2 display intensive dynamics in the top 25 cm of the SAT vadose zone.*
- *Optimal wetting and drying stages are defined according to E_h and gaseous O_2 observations.*
- *The length of wetting and drying stages should be defined separately rather than by adhering to their ratio.*

https://doi.org/10.5194/hess-2021-455
Preprint. Discussion started: 7 October 2021

Hydrology and Earth System Sciences
Discussions
Open Access
EGU

Abstract

Soil aquifer treatment (SAT) is a tertiary process for wastewater treatment where the wastewater infiltrates through a thick vadose zone for purification and storage in the underneath aquifer. SAT infiltration basins are typically flooded intermittently, while maintaining a fixed ratio between the wetting and the drying stages. However, infiltration basins exhibit different physical and chemical properties, limiting the generalization of SAT operation to attain optimal efficiency. Since frequent sampling of the soil pore water to verify the SAT's biodegradation efficiency can be arduous, continuous monitoring of the SAT vadose zone's physico-chemical conditions is required. In this study, redox potential (E_h) was continuously monitored, together with other variables such as water content (θ), soil temperature, and gaseous oxygen (O_2), at multiple depths of a SAT vadose zone throughout the year and while the system was constrained to different operational modes. Hydrological models were calibrated and validated to water content observations, and they illustrated the seasonal changes in water infiltration. Furthermore, it was shown that under long wetting stages during winter, there was a reduction in the SAT's drainage capabilities. The E_h observations, under long wetting stages, demonstrated larger variability and very negative values as ambient temperature increased. Assembling the daily E_h observations illustrated that a wetting stage should cease after about 30 hours, once suboxic conditions are established. A drying stage's optimal duration should be 36 hours, according to the E_h and O_2 observations during summer and winter. Ultimately, the study shows that the length of wetting and drying stages should be defined separately, rather than by adhering to the wetting/drying ratio.

https://doi.org/10.5194/hess-2021-455
Preprint. Discussion started: 7 October 2021

Hydrology and Earth System Sciences
Discussions

1 Introduction

Worldwide water scarcity has motivated the development of alternative water resources such as the reuse of treated wastewater. Soil aquifer treatment (SAT) is commonly implemented to further improve the recovered water's quality and remove the majority of suspended matter, microorganisms, viruses, and organic and inorganic constituents (Dillon, 2005; Goren et al., 2014; Massmann et al., 2006; Schmidt et al., 2011; Tsangaratos et al., 2017). In SAT systems, the treated wastewater is recharged to the underlying aquifer by surface spreading over infiltration basins. The wastewater is purified mainly through the physical and biochemical processes that occur during water passage through the vadose zone (Dillon, 2005; Elkayam et al., 2015). Although SAT systems have been used for decades (Grinshpan et al., 2021; Bouwer, 2002), the ability to estimate and predict a SAT system's performance is still challenging, and the optimal SAT operation is still under investigation (Ben Moshe et al., 2020; Sharma and Kennedy, 2017).

A major uncertainty in SAT systems concerns the vadose zone processes that play a central role in determining the quality of the water that recharges the aquifer (Elkayam et al., 2015). The chemistry of the percolating wastewater changes due to a combination of several biogeochemical processes, such as organic matter biodegradation, nitrification, sorption, cation exchange, etc. (Amy and Drewes, 2007; Díaz-Cruz and Barceló, 2008; Goren et al., 2014; Miller et al., 2006; Tufenkji et al., 2003). Most of the organic matter is removed by biodegradation (i.e. microbial activity) within the upper two meters of the vadose zone (Drewes, 2009). Nevertheless, the microbial activity is greatly affected by the soil water content, which frequently changes in SAT. Generally, a major challenge in SAT systems is to facilitate the intrusion of O_2, primarily in the gaseous phase, and to enrich the active subsurface with O_2 (Ben Moshe et al., 2020; Massmann et al., 2006).

A consequence of the perturbation in the O_2 supply to SAT is expressed in changes in the redox conditions (Mächler et al., 2013; Rezanezhad et al., 2014). Redox potential or oxidation-reduction potential is a quantitative measure of electron availability, i.e., the tendency of the system to receive or donate electrons (Hinchey and Schaffner, 2005). Substantial changes in SAT systems' redox conditions might lead to the release of undesirable metals, such Fe^{2+} and

https://doi.org/10.5194/hess-2021-455
Preprint. Discussion started: 7 October 2021


Hydrology and Earth System Sciences
Discussions

Mn^{2+} (Goren et al., 2012), and affect the degradation rates of pesticides and pharmaceutical substances (Massmann et al., 2006). Additionally, previous studies have illustrated the possible degradation of groundwater quality due to the emergence of contaminants that leach from the SAT vadose zone under reducing conditions (Asano and Cotruvo, 2004; Massmann et al., 2006; Oren et al., 2007; Sharma and Kennedy, 2017). Redox processes are associated with the degradation of organic matter by terminal electron acceptors or redox couples, such as O_2/H_2O, NO_3/N_2, MnO_2/Mn^{2+}, Fe^{3+}/Fe^{2+}, and SO_4/H_2S, in sequential order from the highest energy yield downwards (Berner, 1981; Froelich et al., 1979; Christensen et al., 2000). The transition between redox conditions is determined by the presence and availability of these electron acceptors/donors. Once the strongest oxidizing species (O_2) is depleted, the next strongest oxidizing species is used (NO_3) and so on. The alternation between oxic (> 400 mV), suboxic (between 400 and -100 mV), and anoxic (-100 mV >) conditions in the vadose zone depends on the arability of the oxidized species (Reedy et al., 2000). In addition, studies have reported on the seasonal (temperature changes) effects on redox conditions, which were attributed to the increase in dissolved oxygen concentrations at low temperatures (Massmann et al., 2006) and the greater microbial activity (i.e., higher O_2 consumption) at higher temperatures (Greskowiak et al., 2006; Kirschbaum, 1995).

An important operational aspect of a SAT system is the intermittent application of the effluents (Sattar, 2016; Sallwey et al., 2020). After the infiltration basin is flooded with wastewater, a drying period is implemented to sustain the SAT's infiltration capacity and biochemical capabilities (Sharma and Kennedy, 2017). The wetting and drying stages, which can be expressed by the wet/dry ratio parameter, have a critical impact on the removal rates of dissolved organic carbon, total nitrogen, and pathogens (Ben Moshe et al., 2020; Morrison et al., 2020; Sharma and Kennedy, 2017). Although the wet/dry ratio can vary depending on location and wastewater quality, it is well accepted that it should be below 1.0 (Sattar, 2016; Sharma and Kennedy, 2017). Nevertheless, infiltration basins behave differently with regard to infiltration rates and clogging. Thus, in many cases, the SAT operational efficiency is limited to the personal experience of the operators and their knowledge of the specific infiltration basin (Sharma and Kennedy, 2017). Note, however, that several studies (e.g., Ben Moshe et al., 2021b) suggest that it is not the wet/dry ratio that should be considered, but specific times for wetting and drying.

https://doi.org/10.5194/hess-2021-455
Preprint. Discussion started: 7 October 2021


Hydrology and Earth System Sciences
Discussions

105 The oxidation-reduction potential (E_h), together with chemical and physical parameters such as
106 water content, soil temperature, O_2 concentration, etc., can be continuously monitored by
107 installing the relevant sensors. Previous studies have implemented the E_h sensor and successfully
108 described, with high temporal resolution, the subsurface chemical conditions in various
109 environments, such as wetlands, the water table (or the capillary fringe), aquifers, etc. (Wallace
110 et al., 2019; McMahon and Chapelle, 2008; Shenker et al., 2005; Silver et al., 2018; Rezanezhad
111 et al., 2014). To improve SAT system performances, the link between the wetting and drying
112 stages and the subsequent redox conditions developed in the subsurface should be established.
113 Thus, in situ monitoring can improve SAT management performance and reduce the subjectivity
114 of the operator. The objective of this study was to examine redox's temporal variability and the
115 way it is affected by changes in volumetric water content, gaseous O_2, and temperature imposed
116 by different operational modes of wetting and drying stages. Furthermore, calibrated and
117 validated hydrological models were used to explore the behavior of water fluxes under different
118 operational modes and seasonal temperature changes. Finally, the optimal lengths of a drying
119 stage and a wetting stage were determined, following the in situ observations.

120

121 **2 Methods**

122 **Study sites**

123 The Dan region reclamation project (Shafdan) reclaims about 125 million m^3 of effluent
124 annually, from the Tel Aviv metropolitan area in Israel. The treatment of effluents occurs in two
125 stages. The first stage involves mechanical-biological treatment, which is based on activated
126 sludge, while in the second stage, the treated water (a secondary effluent) is delivered to
127 infiltration basins, as part of the SAT system, to further improve water quality. Six infiltration
128 basin sites, covering a total area of 1.053 Km^2, are located in central Israel, overlying the coastal
129 aquifer (Figure 1). Each basin is divided into several spreading ponds, about 1500 m^2 each,
130 which are alternately flooded. The vadose zone that underlies the basins is mostly composed of
131 sand, sandy loam soil, and calcareous sandstone layers. Typically, the ponds are flooded for one
132 to two days (max hydraulic head of about 50 cm), followed by two to six days of drainage and
133 soil surface drying. The wetting and drying stages are controlled by the ponds' flooding order,

https://doi.org/10.5194/hess-2021-455
Preprint. Discussion started: 7 October 2021


Hydrology and Earth System Sciences
Discussions

the availability of effluent, and the drying period, which is suggested to be at least 24 h (Icekson-Tal et al., 2003). The basin surface is plowed on a regular basis to break up the developed biocrust and to prevent clogging (see Negev et al. (2020) for details).

Study operation

In this research, two in situ measurement stations were installed in an infiltration pond during 2018 (pond 4103 in the Yavne 1 cluster, Figure 1). Each station was equipped with several sets of sensors at various depths, including time domain transmittance (TDT) probes (Acclima Inc., Idaho, USA), copper-constantan thermocouples (OMEGA Engineering, Inc., Connecticut, USA), oxidation-reduction potential (ORP) electrodes (ELH016 van London Co, Houston, TX, USA), and O_2 percentage probes (ICT02 sensor, ICT Int., Australia). Data were collected at prescribed intervals and logged on a CR1000 data logger (Campbell Scientific, Inc., Logan, UT, USA). In addition, suction cups were installed. In station 1 (Figure 1), the data consisted of volumetric water content (VWC) (θ), soil temperature (T), and ORP (E_h) time series, which were continuously measured every 20 minutes between 28/07/2020 and 10/02/2021 (total of 14,185 values, 197 days, for each variable). The data were obtained at 25, 50, and 100 cm depths. In station 2 (Figure 1), VWC, T, gaseous oxygen (O_2), and E_h were measured every 20 minutes between 08/05/2019 and 20/07/2020. There were about 60 days in which data were not collected in station 2 due to technical issues. The data from station 2 contained 27,222 points of VWC, 29,394 points of O_2, 30,414 points of E_h, and 26,730 points of T measurements. In station 2, the data were collected at 25, 50, 75 and 100 cm depths.

The water quality characteristics of the secondary effluent that flooded the Yavne 1 basin are presented in the *Supporting Information (Figure S1)*. Note that the quality parameter concentrations conform to the updated "Inbar" regulations and the findings of a previous study that surveyed numerous wastewater storage and treatment reservoirs across the country (Kfir et al., 2012). To determine the soil physical properties, undisturbed soil cores were sampled at different depths. Subsequently, flow experiments were carried out to calculate the saturated hydraulic conductivity (Ks) based on Darcy's Law (*Supporting Information, Figure S2*).

https://doi.org/10.5194/hess-2021-455
Preprint. Discussion started: 7 October 2021

Hydrology and Earth System Sciences
Discussions
Open Access
EGU

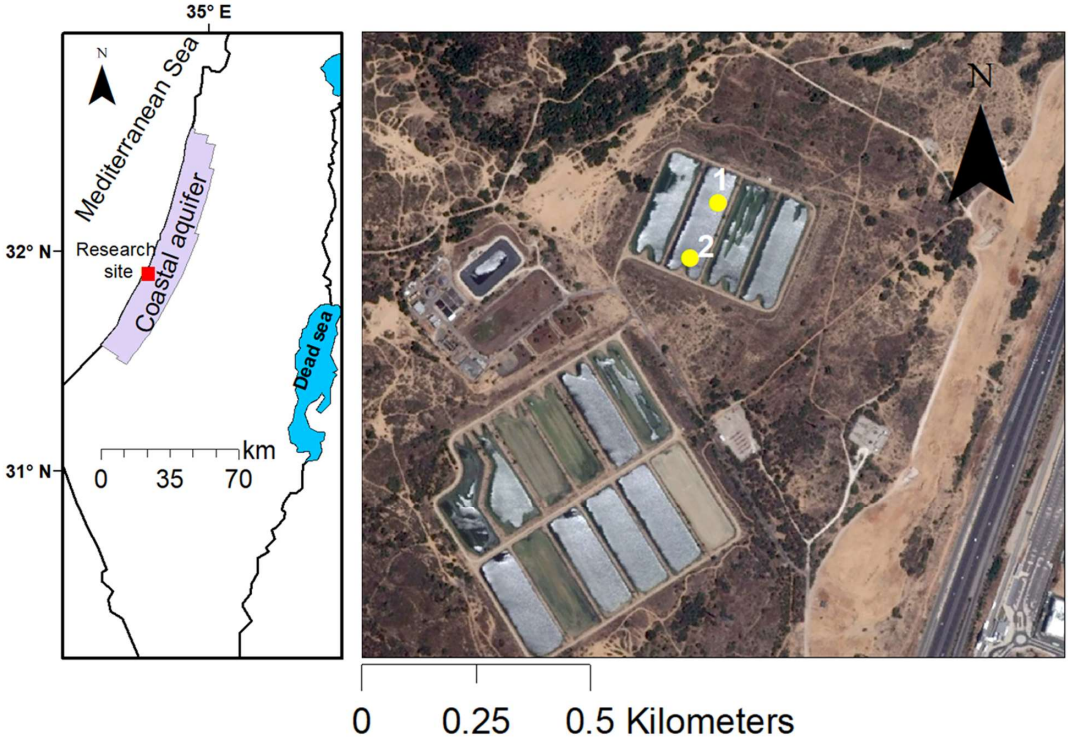

Figure 1: *The location of the investigated site, the Yavne 1 infiltration basin of the Shafdan. In the close up of the investigated pond, the yellow circles represent the locations of the measurement stations (©Google Earth).*

Hydrological model and gaseous oxygen dynamics

The calculations for water and oxygen fluxes in the SAT vadose zone are calculated differently for the ponding stage and for the stage where there is no ponding (water) on the soil surface. For the ponding stage, Ganot et al. (2017) showed that the infiltration rates in managed aquifer recharge systems can be predicted reasonably well by simple analytical models. In this study, a simple model was implemented to calculate the water flux (Bouwer, 2002):

$$q = Ks \times \frac{(L + d - \psi^*)}{L} \quad (1)$$

https://doi.org/10.5194/hess-2021-455
Preprint. Discussion started: 7 October 2021


Hydrology and Earth System Sciences
Discussions

where q (L/T) is the water flux, d (L) is the ponding depth, L (L) is the thickness of the saturated vadose zone, and ψ^* (L) is the negative pressure head at the wetting front. Once the water ponding ceases, the water drainage is set equal to the unsaturated hydraulic conductivity, described with an exponential form (Guswa et al., 2002):

$$D(\theta) = Ks\frac{e^{\beta(\theta-\theta_{fc})}-1}{e^{\beta(\theta_s-\theta_{fc})}-1} \quad (2)$$

where Ks (L/T) is the saturated hydraulic conductivity, β is a parameter of the soil, θ (L^3/L^3) is the VWC, θ_{fc} (L^3/L^3) is the field capacity, and θ_s (L^3/L^3) is the saturated water content (also effective porosity). Furthermore, the effect of temperature changes on the soil hydraulic conductivity is implemented through the change in viscosity (Lin et al., 2003):

$$Ks_T = Ks_{25}\frac{\mu_{25}}{\mu_T} \quad (3)$$

where Ks_T and Ks_{25} are soil hydraulic conductivity values at T°C and 25° C, respectively, and μ_T and μ_{25} are the dynamic viscosity of water (M/LT) values at T° C and 25° C, respectively.

An inverse problem was set to find an optimal combination of Ks and β parameters that minimizes the following objective function:

$$\Phi(b) = \sum_{i=1}^{N}[\theta(t_i) - \theta(t,b)]^2 \quad (4)$$

where N is the number of the VWC observations, $\theta(t_i)$ are the observations at a specific time, and $\theta(t_i,b)$ are the corresponding models' (equations 1-3) predictions for the vector of optimized parameters (b (Ks and β)). The inverse problem was solved using the *fminsearch* function in MATLAB. To evaluate the prediction quality, the root mean squared error (RMSE), the Nash Sutcliffe efficiency (NSE), and the Pearson correlation (r) were calculated following Ritter & Muñoz-Carpena (2013).

https://doi.org/10.5194/hess-2021-455
Preprint. Discussion started: 7 October 2021

Hydrology and Earth System Sciences
Discussions

3 Results and Discussion

The presented data were collected under short and long cycles. The characteristics of the drying and wetting stages are summarized in Table 1. Throughout the analysis described below, we define the winter period as the months between November and April and the summer period as the months between May and October, corresponding to the Mediterranean climate.

Table 1. *Technical information of the recorded long and short wetting and drying cycles*

	Long cycles	Short cycles
Wetting stage (days)	9 ± 2.4	1.5 ± 0.4
Drying stage (days)	3.3 ± 2.4	1.8 ± 1
Number of recorded cycles	33	37
Length of cycle (days)	12.7 ± 3	3.2 ± 1.3
Wet/dry ratio	3 ± 1.8	0.9 ± 0.3

Hydrological conditions

A representative set of VWC (θ) time series measured in the SAT's vadose zone is presented to describe the variability in hydrological conditions measured throughout different seasons and operational modes (Figure 2). The VWC measurements were obtained during long (Figure 2a, b, c) and short (Figure 2d) cycles at three different depths. Note that the water content measurements presented in Figure 2 (a, b) were recorded at station 2 (Figure 1), during summer (Figure 2a) and winter (Figure 2b). The water content variations under short cycles were measured at station 1 (Figure 2c, d). Differences in the absolute values between the water content observations at different depths are mainly related to the vertical texture variability (*Figure S2, Supporting Information*). Under the long cycles, VWC measurements were obtained throughout 19 cycles during summer (May–October) and 14 cycles during winter (November–April). Under short cycles, there were 12 cycles during summer and 25 during winter.

Every recorded wetting event prompted an intensive infiltration that was expressed by a rapid and almost instantaneous increase in water content at all depths and under the two operational

https://doi.org/10.5194/hess-2021-455
Preprint. Discussion started: 7 October 2021


Hydrology and Earth System Sciences
Discussions

modes (Figure 2). Furthermore, the soil remained at high saturation values throughout each wetting stage. Similarly, once the drying process started, it occurred virtually simultaneously at all depths. There were noticeable differences in the drainage rates between summer and winter, where the soil dried faster in summer. To elaborate the drainage process, the drying stages were assembled and averaged at an hourly interval and separated into short (Figure 3a) and long (Figure 3b) cycles. Additionally, equations 1, 2, and 3 (the hydrological model) were implemented to describe the water flow in the SAT's vadose zone under long and short cycles. The hydrological models were calibrated and validated against water content observations at 25 cm depth by adjusting the Ks and β (*Figure S3 and Figure S4, Supporting Information,* Table 2). Throughout the calibration, the Ks and β parameters attained different values for the long cycle periods and the short cycle periods (Table 2). There are differences in soil physical properties between stations 1 and 2, which explains the need for calibrating different parameter sets. In addition, the calibrated Ks values for both models were substantially lower than the measured Ks values (*Figure S2, Supporting Information,* Table 2). It has been shown that Ks measurements in the field are commonly lower than lab Ks measurements (Nimmo et al., 2009). This is related to a reduction in soil conductivity due to air trapping in the soil pores during the wetting process when water is applied at the land surface (Mizrahi et al., 2016; Nimmo et al., 2009).

Under the short cycles, the soil drainage process occurred mostly within the first 15 hours of the drying stage (Figure 3a). The soil drainage rate was slightly higher in summer than in winter. Under the short cycles, the model successfully followed the observed trends, where the validation period showed similar performances (*Figure S3 and* Figure 3a). The model results for the short cycles confirm that the differences in drainage between summer and winter are mainly due to temperature changes that affect water viscosity (Lin et al., 2003). During the long cycle application, the drainage rates in summer showed a moderate VWC decline compared to the observed VWC under short cycles (Figure 3b). This might be due to the differences in soil physical parameters between stations 1 and 2, as highlighted by the calibrated models' parameters (Table 2).

While the model under long cycles successfully followed the drainage trend during summer, the model showed poor performance during winter under long cycles. This is mainly due to the observable changes in VWC measurements, which displayed a shift towards higher values from

https://doi.org/10.5194/hess-2021-455
Preprint. Discussion started: 7 October 2021

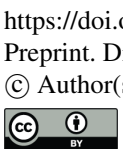

Hydrology and Earth System Sciences
Discussions

November 2019 (*Figure S4 and* Figure 2b). To elaborate the changes in the SAT's physical properties, an additional parameter set was calibrated against the winter data only during the long cycles (Figure 3b, green line). Both the Ks and β parameters attained lower values, and the θ_s increased (*Figure S5 and* Table 2). Previous studies related the accumulation of organic matter in SAT to lower rates of organic matter decomposition during winter (Nadav et al., 2012a). The enrichment in the organic matter in the top layer reduced the soil permeability (Nadav et al., 2012b). It appears that long wetting and drying cycles in SAT during winter can alter the physical soil properties, which eventually affect the infiltration capabilities.

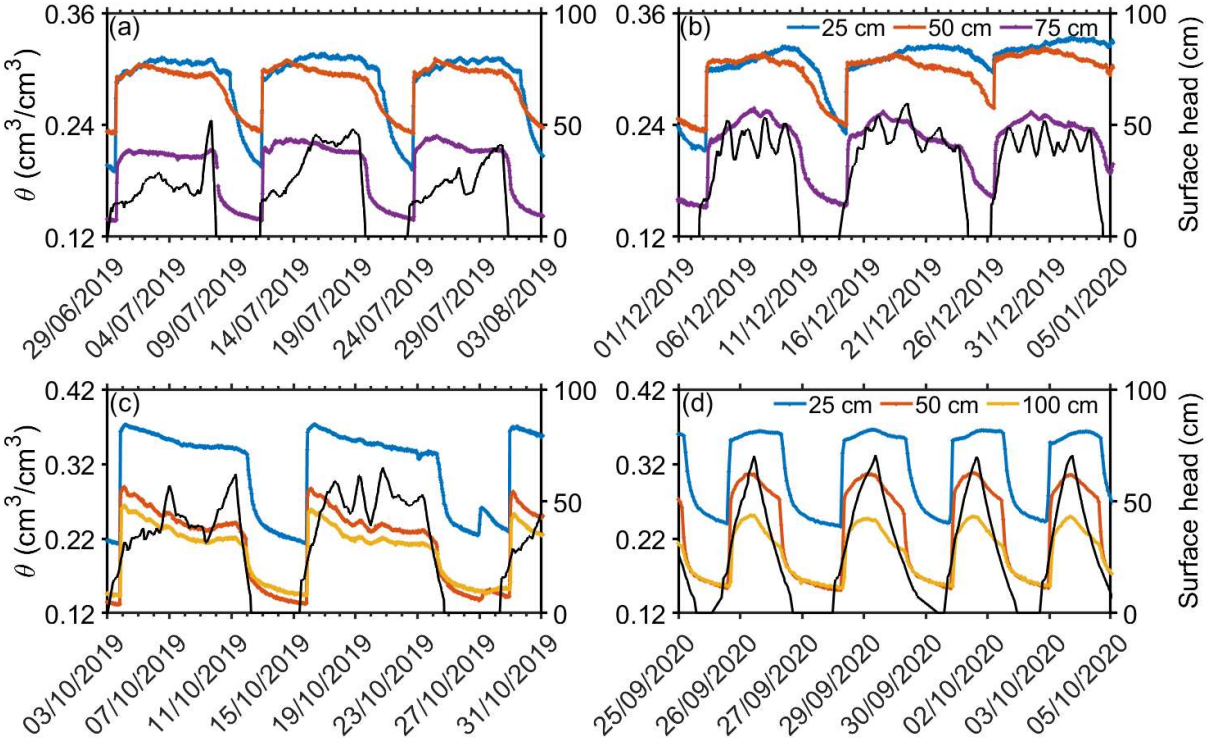

Figure 2: *Representative time series of VWC measurements obtained at station 2 (Figure 1) during (a) summer and (b) winter under long wetting and drying cycles at three different depths. Black line represents*

https://doi.org/10.5194/hess-2021-455
Preprint. Discussion started: 7 October 2021

Hydrology and Earth System Sciences
Discussions

260 *the surface water hydraulic head. The bottom plots display VWC measurements obtained at station 1 under*
261 *(c) long and (d) short wetting and drying cycles during the summer.*

262

263 Table 2. *Estimated parameters of the hydrological models*

	Station 1	Station 2	Station 2 (winter only)
Ks (cm/h)	**5**	**0.9**	**0.72**
θ_s	0.36	0.32	**0.33**
β	**30**	**6.75**	**6.48**
θ_{fc}	0.19	0.19	0.19
ψ^* (cm)	-15	-15	-15
θ_h	0.05	0.05	0.05

264

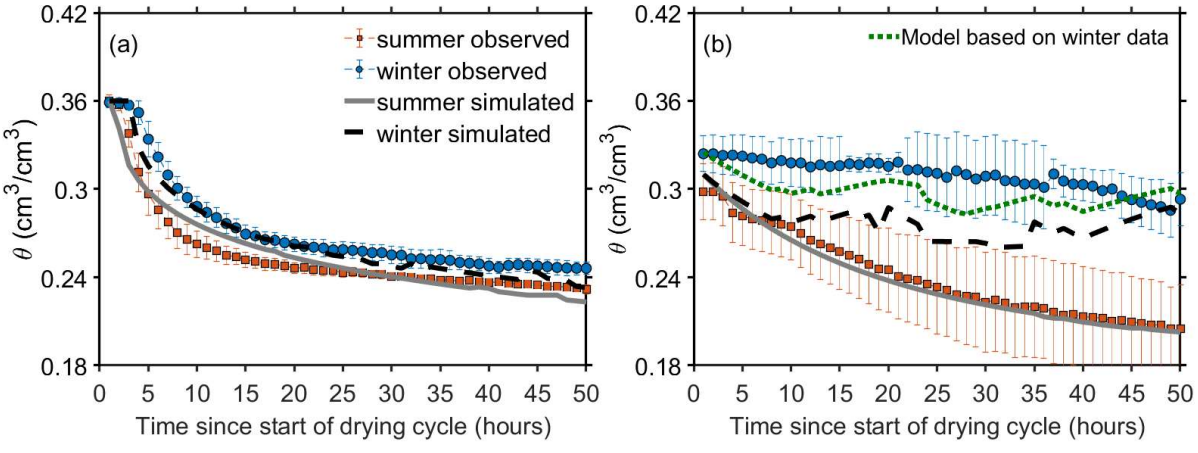

265

266 Figure 3: *The average and standard deviation values of measured VWC at 25 cm depth*
267 *throughout the drying stages at an hourly time scale: (a) short cycles (station 1) and (b) long*
268 *cycles (station 2). The blue and red circles represent the average VWC values collected during*
269 *winter (November–April) and summer (May–October), respectively. The statistics of measured*
270 *VWC under long cycles are based on 19 drying stages during summer and 14 drying stages*
271 *during winter. For the short cycles, the statistics are based on 12 drying stages during summer*

https://doi.org/10.5194/hess-2021-455
Preprint. Discussion started: 7 October 2021


Hydrology and Earth System Sciences
Discussions

and 24 drying stages during winter. The dashed black and solid gray lines represent the average values of simulated VWC throughout the drying stage during winter (November–April) and summer (May–October), respectively. Note that for the long cycle periods, an additional model was established based only on winter data (green line).

Seasonal differences in SAT redox (E_h) conditions under long wetting cycles

E_h conditions were monitored at four depths (Figure 4a, b). The behavior of the E_h dynamic following a wetting event was similar for the summer and the winter periods. At 25, 50, and 75 cm depths, a gradual decline in E_h started only after a time lag from the beginning of a wetting event (Figure 4a, b). This time lag can be explained by the presence of dissolved oxygen (DO) in the percolating solution. Once DO is depleted, suboxic and anoxic conditions begin to develop (Dutta et al., 2015; Ben Moshe et al., 2021, 2020). The E_h conditions at 25 cm were the most highly responsive to the wetting events, while the E_h conditions were the most negative at this depth (Figure 4a, b). At 100 cm depth, only minor changes were observed, and in some cases (during winter), no changes were observed (Figure 4a, b). According to the gaseous O_2 measurements (Figure 4c, d), there were partially aerated conditions during some of the flooding events at 100 cm depth. Therefore, the small changes of E_h at 100 cm depth could either have been the outcome of only minor biochemical activity, or they could have been due to the sufficient oxygen supply. Furthermore, the monitored E_h conditions illustrate that most of the activity in SAT systems occurs at the topsoil, as illustrated in previous studies (e.g., Quanrud et al., 1996, 2003; Sopilniak et al., 2017). Note that the E_h recovery time, i.e., an increase towards positive values, was virtually instantaneous once the drying process initiated (Figure 4a, b). The increase in E_h conditions occurred concurrently with the observed rapid increase of the gaseous oxygen (O_2) in the vadose zone (Figure 4c, d).

A distinct difference in E_h conditions between winter and summer at 25 cm depth is expressed by a more negative range of values during summer (Figure 4a, b). Since similar wastewater quality and hydraulic loads were fed to the pond during summer and winter (*Supporting Information*), the E_h conditions were mainly affected by the SAT's aeration state and seasonal temperature changes. In Figure 5, the monthly E_h conditions at 25 cm depth are presented in the form of a boxplot, together with the monthly average ambient temperature (dashed black line) and monthly

https://doi.org/10.5194/hess-2021-455
Preprint. Discussion started: 7 October 2021


Hydrology and Earth System Sciences
Discussions

average global radiation (gray line). The E_h conditions showed a wider range of values with the increase in temperature (Figure 5). Between November and March, the E_h conditions mostly remained above zero or were slightly negative (Figure 5). Once the temperature increased above 24°C between May and October, E_h conditions showed substantial fluctuation between negative and positive values (Figure 5). Note that the average monthly ambient temperatures during November and May were similar in value, but during November, the E_h conditions mostly remained above zero (Figure 5). This difference is connected to the daylight duration, as indicated by the global radiation, which is substantially greater in May than in November (Figure 5, gray line). A typical characteristic of aquatic systems is the large fluctuations in dissolved oxygen (DO) concentrations due to intense photosynthesis and respiration (Stumm, W., & Morgan, 1996). Goren et al. (2014) illustrated that following the effluent spreading in the infiltration ponds, photosynthesis enriches the water with DO. Furthermore, chemical analysis of porewater samples that were obtained at 0.5 m depth in the SAT vadose zone indicated DO's substantial influence on the biochemical conditions of the percolating water (Goren et al., 2014). Thus, the photosynthesis process enriches the effluent with DO, which encourages further microbial activity (Goren et al., 2014; Hargreaves, 2006; Rodríguez-Escales et al., 2020). However, between July and September, there was a decrease in global radiation that did not affect the E_h variability (Figure 5). Thus, it appears that under long wetting stages, the seasonal temperature changes dominate the E_h conditions but show some trade-off with the global radiation.

https://doi.org/10.5194/hess-2021-455
Preprint. Discussion started: 7 October 2021

Hydrology and Earth System Sciences
Discussions
Open Access
EGU

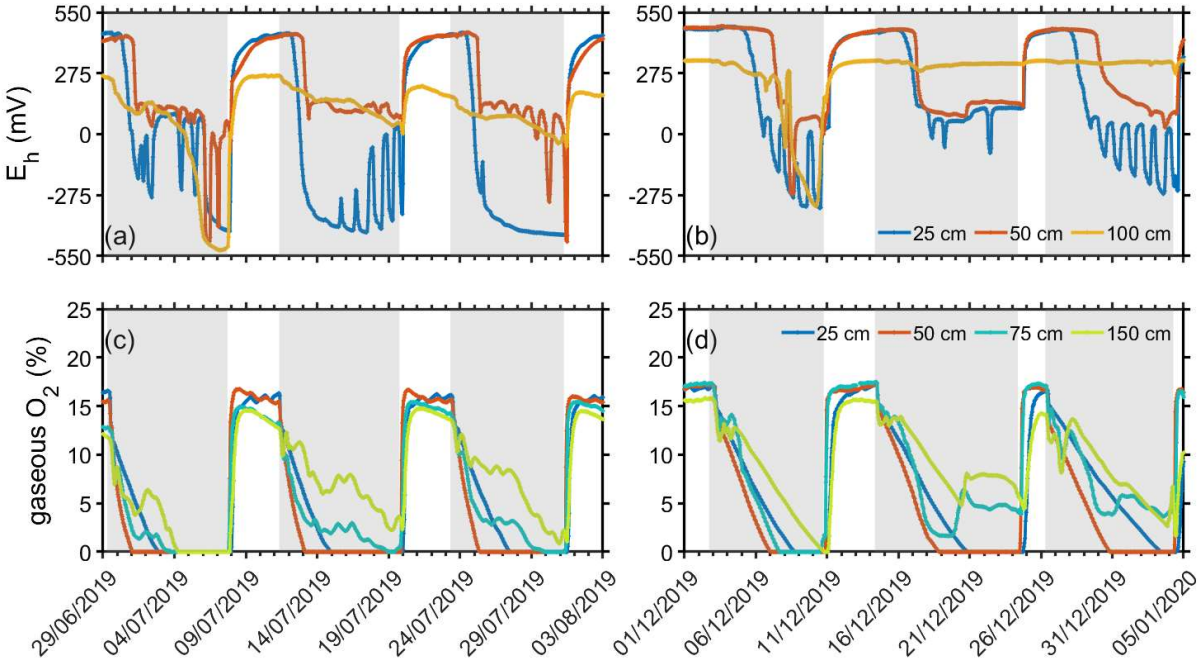

322

323 Figure 4: *Representative time series of redox-potential (E_h) and gaseous O_2 measurements*
324 *obtained at station 2 (Figure 1) at depths of 25, 50, and 100 cm: (a, c) summer and (b, d) winter.*
325 *Note that the gray and white areas indicate wetting and drying periods, respectively.*

326

https://doi.org/10.5194/hess-2021-455
Preprint. Discussion started: 7 October 2021

Hydrology and Earth System Sciences
Discussions

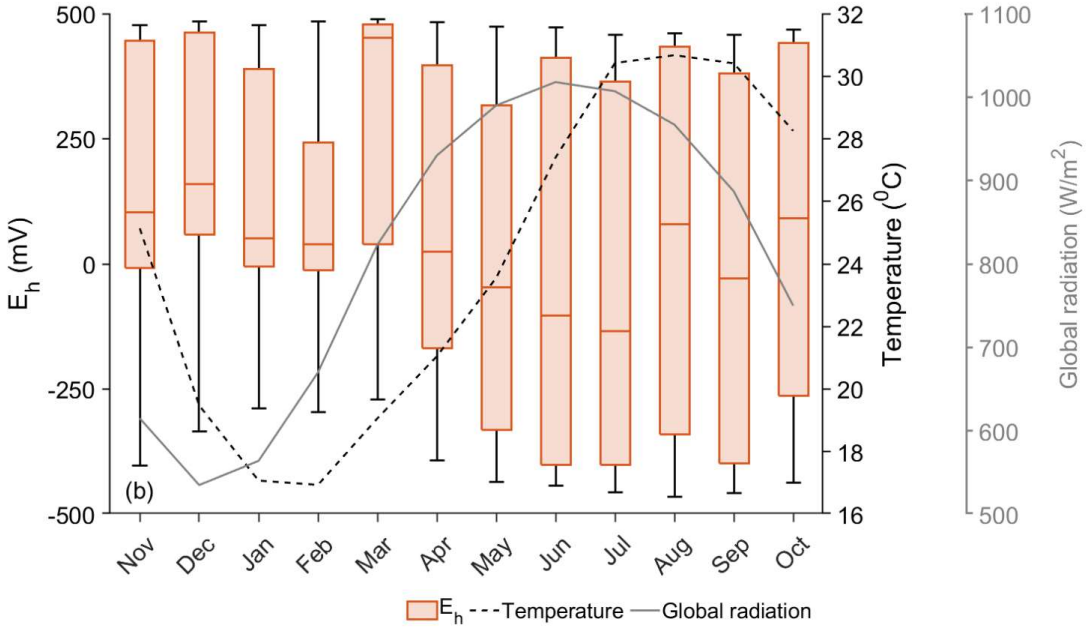

Figure 5: *Seasonal changes in E_h conditions as were observed at 25 cm depth at station 2 under long (seven days) wetting periods. The dashed black line represents the monthly mean ambient temperature, and the solid gray line represents the monthly mean global radiation obtained from the Israeli Meteorological Service (IMS, 2021).*

A comparison between SAT redox (E_h) conditions under long and short cycles

It has been shown that the operational mode affects the aeration conditions of the upper vadose zone, which consequently might alter the infiltration rates and the intensity of the biogeochemical processes (Goren et al., 2014). Throughout the measurement period, the intervals of wetting and drying stages were modified (Table 1). The wetting and drying stages were substantially shortened during September 2020, which enabled examining the differences in E_h conditions under short and long cycles. The variations in E_h conditions under long cycles during October 2019, December 2019, and January 2020 are presented in Figure 6a, c. In addition, the changes in E_h conditions under short cycles during September–October 2020, December 2020, and January 2021 are presented in Figure 6b, d.

https://doi.org/10.5194/hess-2021-455
Preprint. Discussion started: 7 October 2021


Hydrology and Earth System Sciences
Discussions

As was shown above, under long cycles, the E_h conditions declined towards slightly negative values during winter and attained markedly negative values during the summer months at 25 and 50 cm depths, where only minor variations were observed at 100 cm depth (Figure 6a, c). The E_h conditions, under short cycles during the summer, showed a decline towards slightly negative values for a brief time compared to long cycles (Figure 6a, b). During the winter, only minor variations in E_h conditions were recorded under short cycles (Figure 6d). Note that at 100 cm depth, there was almost no change in E_h conditions for either season under short cycles (Figure 6b, d). As was illustrated previously (Figure 4a, b), once the drying stage initiated, the recovery of E_h towards positive values (oxic conditions) was almost instant under both short and long cycles. It appears that the re-establishment of oxic conditions occurs independently of the length of the wetting stage.

The observations of E_h and gaseous O_2 under long and short cycles indicate a weak relationship between the wetting and the drying stages. These results call into question the advantage of implementing the wet/dry ratio for optimizing SAT performance. It appears that the length of a wetting stage and a drying stage should be defined separately (Ben Moshe et al., 2020, 2021). Thus, the necessary further investigation is described below to examine the optimal lengths of the wetting and drying stages.

https://doi.org/10.5194/hess-2021-455
Preprint. Discussion started: 7 October 2021

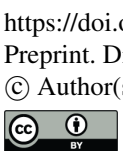

Hydrology and Earth System Sciences
Discussions

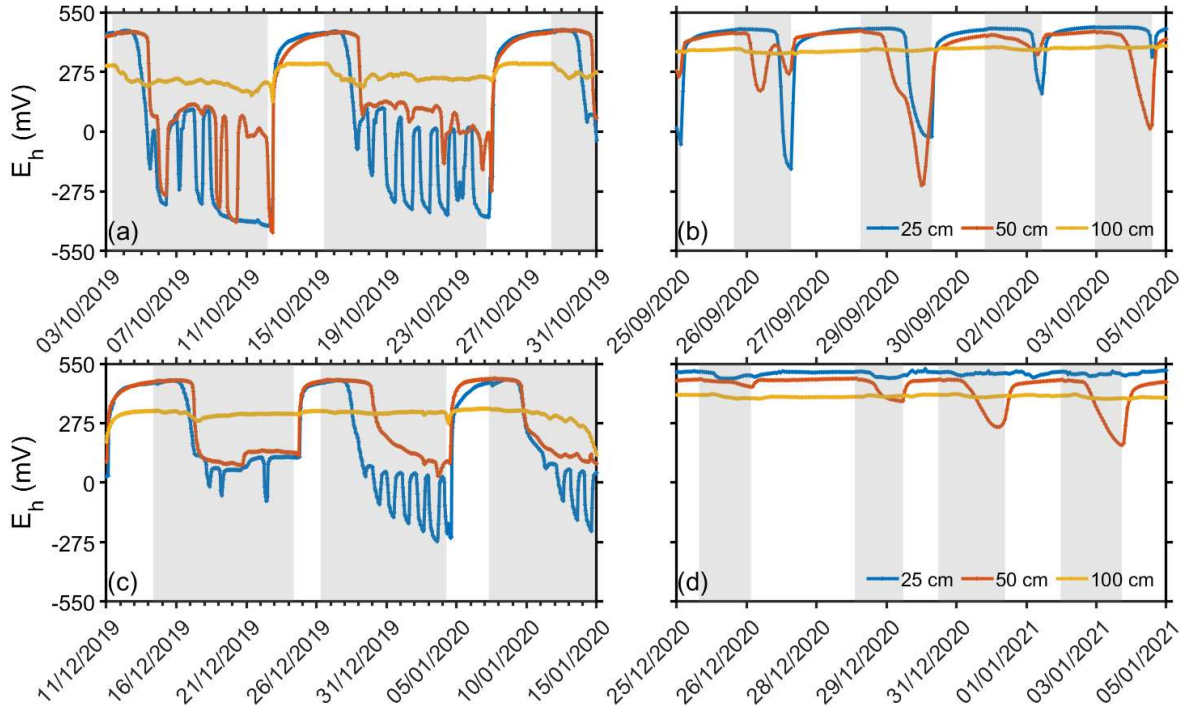

Figure 6: *Representative time series of redox-potential (E_h) measurements at 25, 50 and 100 cm depths in station 1 (Figure 1): (a, c) long wetting periods and (b, d) short wetting periods. Note that the gray and white areas indicate wetting and drying periods, respectively.*

The length of the wetting stage according to E_h measurements

During wetting stages, the main limiting factor of the biodegradation process is the availability of dissolved oxygen (Skopp et al., 1990; Cook and Knight, 2003). Once the soil pores are fully saturated, only the dissolved oxygen (DO) of the percolating water is available. However, studies have illustrated that the DO of the percolating water rapidly depletes (Dutta et al., 2015; Ben Moshe et al., 2021, 2020). Thus, the wetting stage should cease when the DO no longer has an effect on the degradation process, i.e., when suboxic and anoxic conditions begin to develop. E_h measurements can provide a good indication for the time when such conditions begin to be established. For this purpose, the hourly measured E_h conditions during the wetting stage of 33 recorded cycles (19 cycles during summer and 14 cycles during winter) were averaged (Figure 7). The data were separated between winter (November–April) and summer (May–October),

https://doi.org/10.5194/hess-2021-455
Preprint. Discussion started: 7 October 2021


Hydrology and Earth System Sciences
Discussions

according to the trends presented in Figure 5. Since the data showed large variability for both seasons (Figure 7), a two-sample t-test (ttest2 function of Matlab) was used to test whether the E_h measurements during winter and summer came from distributions with equal means at the 95% significance level for each hour interval. The test indicated that after 28 hours of wetting, the E_h averages during winter became significantly different than the summer E_h averages.

During summer, the decline in E_h conditions was steeper compared to the trend exhibited in winter (Figure 7). Following 40 hours of wetting, the E_h conditions during the summer dropped below 100 mV, which indicates the establishment of considerable suboxic conditions (Figure 7). After 48 hours, the E_h observations suggested that anoxic conditions prevailed in the vadose zone (Figure 7). Thus, during the summer months, the optimal length of a wetting stage, in terms of biodegradation, would be no more than about 30 hours (1.25 day^{-1}). At this length of time, there is a minor risk that anoxic conditions would develop. This is in agreement with Dutta et al. (2015), who suggested a relatively wide distribution of de-oxygenation times, between 0.36 and 1.5 day^{-1}.

In winter, the E_h measurements indicated that the wetting stage should cease only after 80 hours (establishment of anoxic conditions, Figure 7). However, this inference might be misleading since there is a trade-off between nutrient transport rates and reaction rates (Greskowiak et al., 2006). Although the low temperatures enable higher DO, the microbial activity is slower (Kirschbaum, 1995). That is, the delay in E_h drop (compared to summer) is due to lower oxygen demand. Assuming that the nutrient transport is mainly advective, at intensive infiltration rates during winter, the supply of the percolated effluent's substrate might be faster than the SAT's degradation capability. Therefore, determining the length of a wetting stage during winter, using solely the E_h measurements, may be challenging. As indicated by the two-sample t-test results, the differences between summer and winter E_h values in the first 28 hours of wetting are insignificant. Therefore, for practical purposes, the length of a wetting stage during winter should be no more than 30 hours, as in the summer period.

https://doi.org/10.5194/hess-2021-455
Preprint. Discussion started: 7 October 2021

Hydrology and Earth System Sciences
Discussions

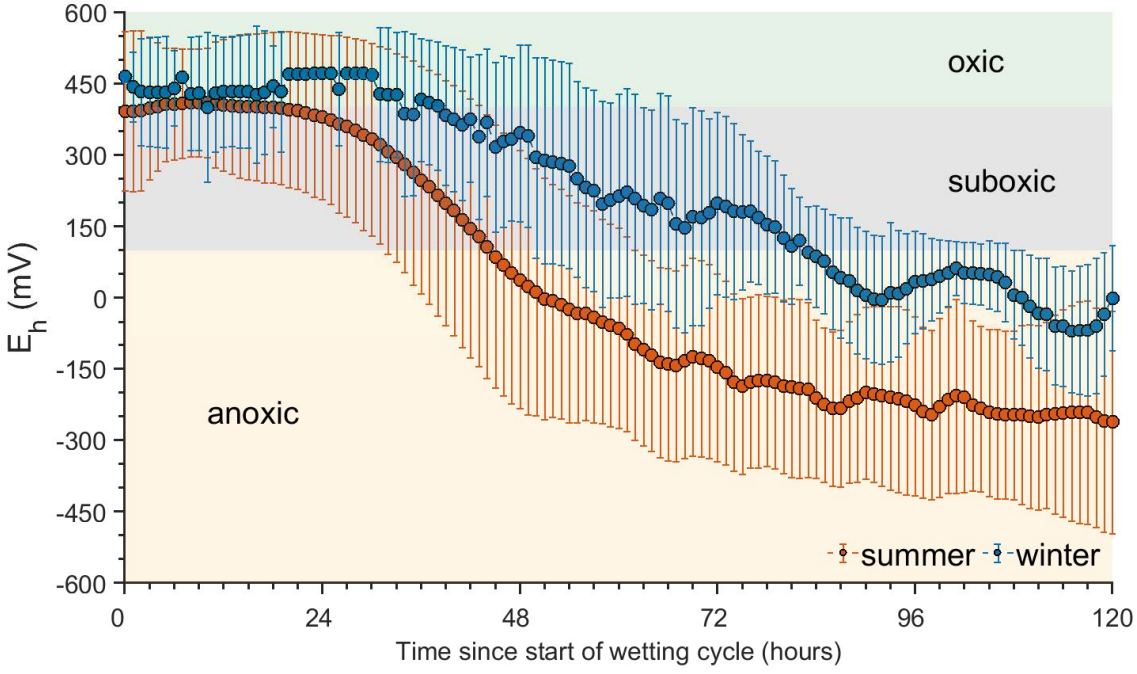

Figure 7: *Plot of hourly means of E_h measurements from the beginning of the wetting stages. The statistics are based on 19 cycles during summer (May–October) and 14 cycles during winter (November–April) that were observed at 25 cm depth in station 2. Note that the data are separated between summer and winter according to the trends presented in* Figure 5*. The green, grey, and yellow areas represent the oxic (400mV <), suboxic (400mV > E_h > 100mV), and anoxic E_h < 100mV) conditions, respectively.*

The length of the drying stage using E_h and gaseous O_2 measurements

The drying stage in SAT systems is implemented to restore the infiltration, biological, and chemical capabilities of the pond, mainly by aerating the soil (Sharma and Kennedy, 2017). A drying stage is defined as the stage in which there is no water at the soil surface, and the observed VWCs begin to decrease (Figure 2). To determine the optimal time for a drying stage, both the measured E_h and gaseous O_2 observations that were obtained at 25 cm depth during the drying stages were averaged (Figure 8 and Figure 9).

https://doi.org/10.5194/hess-2021-455
Preprint. Discussion started: 7 October 2021

Hydrology and Earth System Sciences
Discussions

Following the analysis presented in Figure 7, the E_h data during the drying stages were also separated between winter (November–April) and summer (May–October), according to the trends presented in Figure 5. A two-sample t-test at the 95% significance level was conducted for the E_h measurements during winter and summer for each hourly interval. The test indicated that for the first 20 hours of the drying stage, the E_h averages during winter were significantly different than the E_h averages during summer. These results verify that the E_h conditions at the beginning of the drying stage during the summer period were much more negative than during winter (Figure *8*). Thus, the recovery of the E_h conditions towards suboxic conditions occurred at faster rate (~12 hours) than the recovery during summer, i.e., about 18 hours (Figure 8). Nevertheless, the E_h observations illustrate that the re-establishment of oxic conditions in the SAT vadose zone is similar during the winter and summer periods (Figure 8). Once the drying stage started, it required about 36 hours for the E_h conditions to reach values in the range of oxic conditions, regardless of the initial value of the E_h conditions (Figure 8).

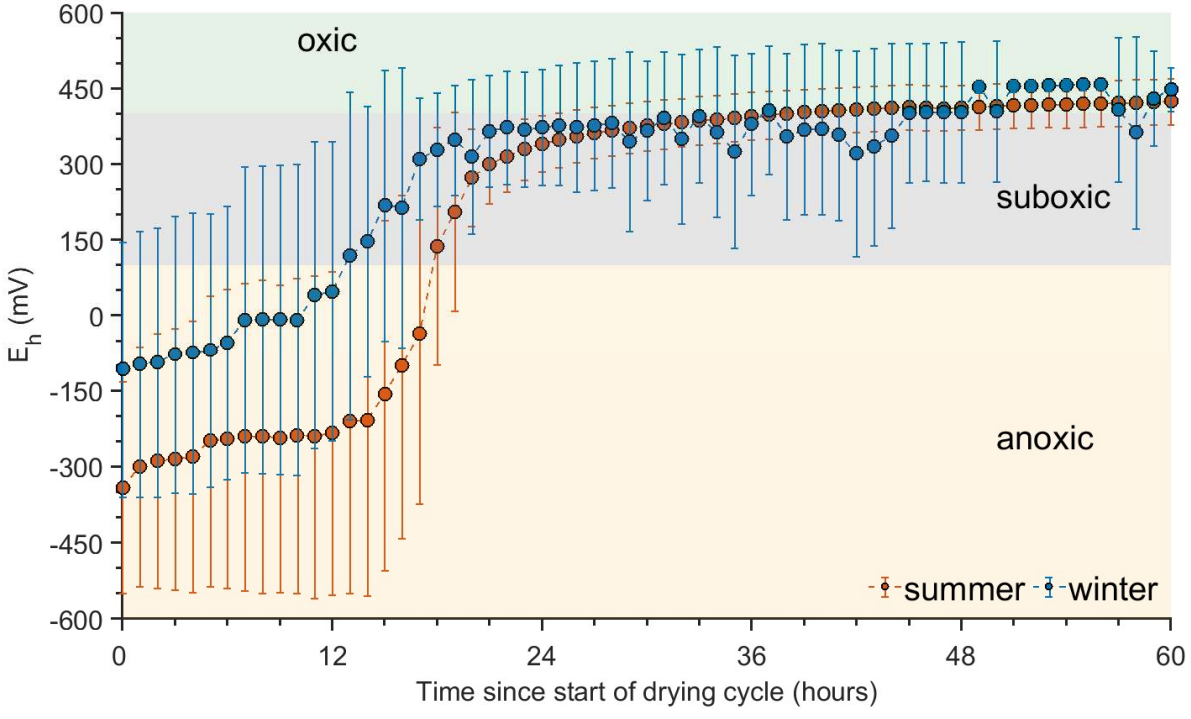

https://doi.org/10.5194/hess-2021-455
Preprint. Discussion started: 7 October 2021


Hydrology and Earth System Sciences
Discussions

435 Figure 8: *Plot of hourly means of E_h measurements from the beginning of the drying stages. The statistics*
436 *are based on 19 cycles during summer (May–October) and 14 cycles during winter (November–April)*
437 *that were observed at 25 cm depth in station 2. Note that the data are separated between summer and*
438 *winter according to the trends presented in* Figure 5. *The green, grey, and yellow areas represent the oxic*
439 *(400mV <), suboxic (400mV > E_h > 100mV), and anoxic E_h < 100mV) conditions, respectively.*

440 Figure 9 presents the average gaseous O_2 concentrations at different times from the beginning of
441 the drying stage during summer (Figure 9a) and winter (Figure 9b). The different colors indicate
442 the times from the beginning of drying (Figure 9). Rapid aeration rates were observed during
443 summer compared to winter. For example, after 16 hours of drying, the gaseous O_2
444 concentrations during summer reached 13% (Figure 9a), while during winter, the concentrations
445 were about 4.5% (Figure 9b). Note that after 22 hours of drying during summer, the aeration rate
446 declined substantially, and only a minor increase in gaseous O_2 concentrations was observable
447 (Figure 9a). During winter, the gaseous O_2 concentrations reached 14% only after 37 hours
448 (Figure 9b). Thus, the aeration of the SAT vadose zone requires almost double the time during
449 winter than during summer.

450 The results presented in Figure 9 call into question the E_h observations during the drying stage
451 (Figure 8), which indicate that the drying cycle should be about 36 hours for both winter and
452 summer. One would expect that intensive aeration rates of the vadose zone during summer
453 would result in a faster recovery of the E_h conditions. However, a recent study has indicated that
454 using solely the gaseous O_2 concentration to quantify soil aeration status might be inaccurate for
455 some conditions (Ben-Noah et al., 2021). Instead, the authors suggested using the Damkholer
456 number, which is the ratio between characteristic diffusion (i.e., oxygen supply) and soil
457 respiration times. A small Damkholer number would be calculated when the O_2 consumption rate
458 is lower than the O_2 supply. Thus, although during summer, the oxygen supply rate is relatively
459 high compared to winter (Figure 9), the oxygen consumption rate for soil respiration is expected
460 to be substantially higher during summer than during winter (Kirschbaum, 1995).

461

https://doi.org/10.5194/hess-2021-455
Preprint. Discussion started: 7 October 2021

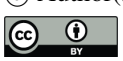

Hydrology and Earth System Sciences
Discussions

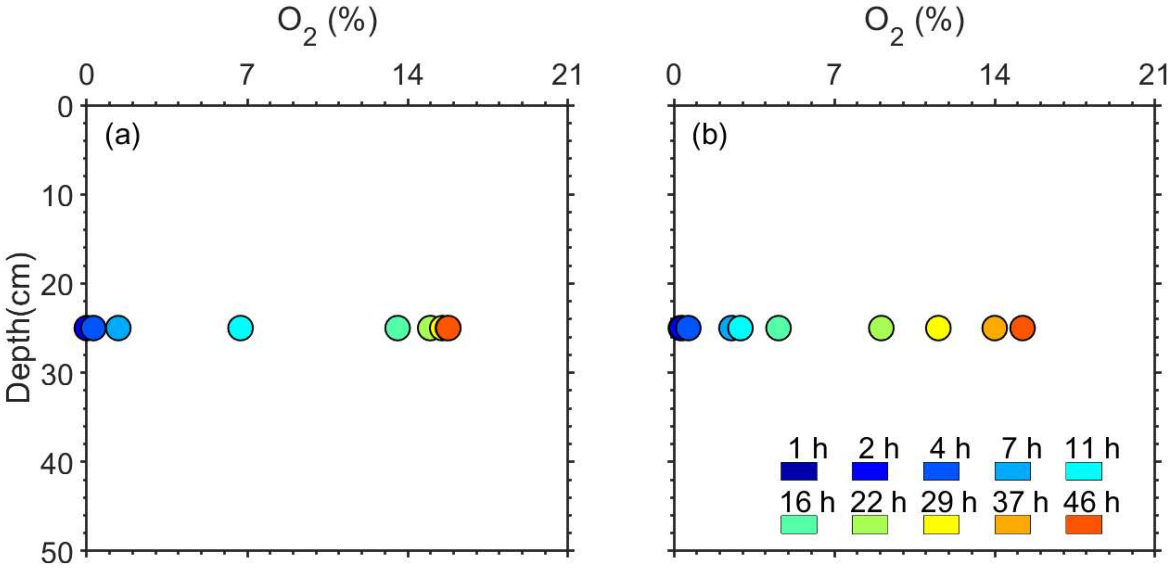

462

463 Figure 9: *Temporal distribution of the measured (dots at 25 cm depth) of gaseous O_2*
464 *concentrations in the SAT vadose zone during the drying stage (note that the colors indicate*
465 *different times from the initiation of drying stage) for: (a) summer and (b) winter.*

466

467 **4 Summary and Conclusions**

468 Continuous monitoring of redox conditions (E_h), VWC (θ), temperature (T), and gaseous O_2 in
469 the vadose zones of SAT infiltration ponds was carried out for about 600 days. SAT operation
470 was subjected to long and short wetting and drying cycles and seasonal changes. The datasets
471 enabled the examination of factors that control the hydrological and geochemical conditions in
472 SAT. Calibrated and validated hydrological models were applied to investigate the water flow
473 dynamics in the SAT vadose zone. E_h and gaseous O_2 observations were averaged to determine
474 seasonal changes and deduce the optimal length of wetting and drying stages.

475 The examination of the measured E_h conditions illustrated a noticeable decline to markedly
476 negative values (-450mV >) during summer and to values between 0 and -50 mV during winter.
477 These E_h conditions were established following 30 hours of wetting, and no considerable
478 changes in E_h conditions were noticeable until the wetting stages ceased. A monthly statistic of

https://doi.org/10.5194/hess-2021-455
Preprint. Discussion started: 7 October 2021


Hydrology and Earth System Sciences
Discussions

the E_h measurements illustrated the relationship between the size of the E_h amplitude and the seasonal T changes. Furthermore, it is speculated that the limited decrease in E_h conditions during winter were due to lower microbial activity. An additional support for this claim is the reduction in infiltration capabilities following long wetting and drying cycles during winter, as was indicated by the hydrological models. To define the optimal length of a wetting stage, the E_h data were averaged and separated between the winter and summer periods. During the summer period, the optimal time length of a wetting stage, according to E_h observations, is about 30 hours. Determining the optimal length of a wetting stage during winter is challenging. Practically, there are no significant differences between E_h conditions during winter and summer for the first 28 hours of wetting. Thus, the length of a wetting stage during winter should be 30 hours, as in the summer period.

The length of a drying stage, following the E_h observations, should be about 36 hours, regardless of the initial values of the E_h conditions and the season. Note that during summer, a longer drying time is required for the E_h conditions to attain suboxic conditions. Nevertheless, the gaseous O_2 observations indicated faster aeration rates during summer, which compensate for the very negative E_h conditions and allow fast recovery. Following our analysis, we suggest that under the tested conditions, the length of a drying stage should be 36 hours for winter and summer. Shorter drying stages would affect SAT efficiency, while applying longer drying stages would reduce the total hydraulic loads that can be fed to the infiltration basin.

Implementing in situ E_h, VWC, T and gaseous O_2 sensors provided continuous high-resolution observations. These datasets revealed the hydrological and biochemical dynamics in SAT as imposed by seasonal and operational changes. Analysis of the E_h and O_2 measurements enabled the identification of the optimal time lengths of wetting and drying stages. The results indicated that there is no direct relationship between the length of a wetting stage and a drying stage. Thus, the operational use of a wetting/drying ratio in SAT management should be reconsidered.

Acknowledgments

This work was financed within the framework of the German–Israeli Water Technology Cooperation Program under Project No. WT1601/2689, by the German Federal Ministry of

https://doi.org/10.5194/hess-2021-455
Preprint. Discussion started: 7 October 2021

Hydrology and Earth System Sciences
Discussions
Open Access
EGU

508 Education and Research (BMBF), and by the Israel Ministry of Science, Technology and Space
509 (MOST).

https://doi.org/10.5194/hess-2021-455
Preprint. Discussion started: 7 October 2021


Hydrology and Earth System Sciences
Discussions

References

Amy, G. and Drewes, J.: Soil aquifer treatment (SAT) as a natural and sustainable wastewater reclamation/reuse technology: Fate of wastewater effluent organic Matter (EfoM) and trace organic compounds, Environ. Monit. Assess., 129, 19–26, https://doi.org/10.1007/s10661-006-9421-4, 2007.

Asano, T. and Cotruvo, J. A.: Groundwater recharge with reclaimed municipal wastewater: Health and regulatory considerations, Water Res., 38, 1941–1951, https://doi.org/10.1016/j.watres.2004.01.023, 2004.

Ben-Noah, I., Nitsan, I., Cohen, B., Kaplan, G., and Friedman, S. P.: Soil aeration using air injection in a citrus orchard with shallow groundwater, Agric. Water Manag., 245, 106664, https://doi.org/10.1016/j.agwat.2020.106664, 2021.

Berner, R. A.: A new geochemical classification of sedimentary environments, J. Sediment. Perology, 51, 359–365, https://doi.org/https://doi.org/10.1306/212F7C7F-2B24-11D7-8648000102C1865D, 1981.

Bouwer, H.: Artificial recharge of groundwater: Hydrogeology and engineering, Hydrogeol. J., 10, 121–142, https://doi.org/10.1007/s10040-001-0182-4, 2002.

Christensen, T. H., Bjerg, P. L., Banwart, S. A., Jakobsen, R., Heron, G., and Albrechtsen, H. J.: Characterization of redox conditions in groundwater contaminant plumes, J. Contam. Hydrol., 45, 165–241, https://doi.org/10.1016/S0169-7722(00)00109-1, 2000.

Cook, F. J. and Knight, J. H.: Oxygen Transport to Plant Roots, Soil Sci. Soc. Am. J., 67, 20–31, https://doi.org/10.2136/sssaj2003.2000, 2003.

Díaz-Cruz, M. S. and Barceló, D.: Trace organic chemicals contamination in ground water recharge, Chemosphere, 72, 333–342, https://doi.org/10.1016/j.chemosphere.2008.02.031, 2008.

Dillon, P.: Future management of aquifer recharge, Hydrogeol. J., 13, 313–316, https://doi.org/10.1007/s10040-004-0413-6, 2005.

Drewes, J. E.: Ground water replenishment with recycled water - Water quality improvements during managed aquifer recharge, Ground Water, 47, 502–505, https://doi.org/10.1111/j.1745-

537 6584.2009.00587_5.x, 2009.

538 Dutta, T., Carles-Brangarí, A., Fernàndez-Garcia, D., Rubol, S., Tirado-Conde, J., and Sanchez-
539 Vila, X.: Vadose zone oxygen (O2) dynamics during drying and wetting cycles: An artificial
540 recharge laboratory experiment, J. Hydrol., 527, 151–159,
541 https://doi.org/10.1016/j.jhydrol.2015.04.048, 2015.

542 Elkayam, R., Sopliniak, A., Gasser, G., Pankratov, I., and Lev, O.: Oxidizer Demand in the
543 Unsaturated Zone of a Surface-Spreading Soil Aquifer Treatment System, Vadose Zo. J., 14,
544 vzj2015.03.0047, https://doi.org/10.2136/vzj2015.03.0047, 2015.

545 Froelich, P. N., Klinkhammer, G. P., Bender, M. L., Luedtke, N. A., Heath, G. R., Cullen, D.,
546 Dauphin, P., Hammond, D., Hartman, B., and Maynard, V.: Early oxidation of organic matter in
547 pelagic sediments of the eastern equatorial Atlantic: suboxic diagenesis, Geochim. Cosmochim.
548 Acta, 43, 1075–1090, https://doi.org/10.1016/0016-7037(79)90095-4, 1979.

549 Ganot, Y., Holtzman, R., Weisbrod, N., Nitzan, I., Katz, Y., and Kurtzman, D.: Monitoring and
550 modeling infiltration-recharge dynamics of managed aquifer recharge with desalinated seawater,
551 Hydrol. Earth Syst. Sci., 21, 4479–4493, https://doi.org/10.5194/hess-21-4479-2017, 2017.

552 Goren, O., Lazar, B., Burg, A., and Gavrieli, I.: Mobilization and retardation of reduced
553 manganese in sandy aquifers: Column experiments, modeling and implications, Geochim.
554 Cosmochim. Acta, 96, 259–271, https://doi.org/10.1016/j.gca.2012.06.032, 2012.

555 Goren, O., Burg, A., Gavrieli, I., Negev, I., Guttman, J., Kraitzer, T., Kloppmann, W., and Lazar,
556 B.: Biogeochemical processes in infiltration basins and their impact on the recharging effluent,
557 the soil aquifer treatment (SAT) system of the Shafdan plant, Israel, Appl. Geochemistry, 48,
558 58–69, https://doi.org/10.1016/j.apgeochem.2014.06.017, 2014.

559 Greskowiak, J., Prommer, H., Massmann, G., and Nützmann, G.: Modeling seasonal redox
560 dynamics and the corresponding fate of the pharmaceutical residue phenazone during artificial
561 recharge of groundwater, Environ. Sci. Technol., 40, 6615–6621,
562 https://doi.org/10.1021/es052506t, 2006.

563 Grinshpan, M., Furman, A., Dahlke, H. E., Raveh, E., and Weisbrod, N.: From managed aquifer
564 recharge to soil aquifer treatment on agricultural soils: Concepts and challenges, Agric. Water

565 Manag., 255, 106991, https://doi.org/10.1016/j.agwat.2021.106991, 2021.

566 Guswa, A. J., Celia, M. A., and Rodriguez-Iturbe, I.: Models of soil moisture dynamics in
567 ecohydrology: A comparative study, Water Resour. Res., 38, 5-1-5–15,
568 https://doi.org/10.1029/2001wr000826, 2002.

569 Hargreaves, J. A.: Photosynthetic suspended-growth systems in aquaculture, Aquac. Eng., 34,
570 344–363, https://doi.org/10.1016/j.aquaeng.2005.08.009, 2006.

571 Hinchey, E. K. and Schaffner, L. C.: An evaluation of electrode insertion techniques for
572 measurement of redox potential in estuarine sediments, Chemosphere, 59, 703–710,
573 https://doi.org/10.1016/j.chemosphere.2004.10.029, 2005.

574 Icekson-Tal, N., Avraham, O., Sack, J., and Cikurel, H.: Water reuse in Israel – the Dan region
575 project: evaluation of water quality and reliability of plant's operation., 3, 231–237, 2003.

576 Kfir, O., Tal, A., Gross, A., and Adar, E.: The effect of reservoir operational features on recycled
577 wastewater quality, Resour. Conserv. Recycl., 68, 76–87,
578 https://doi.org/10.1016/j.resconrec.2012.08.002, 2012.

579 Kirschbaum, M. U. F.: The temperature dependence of soil organic matter decomposition, and
580 the effect of global warming on soil organic C storage, Soil Biol. Biochem., 27, 753–760,
581 https://doi.org/10.1016/0038-0717(94)00242-S, 1995.

582 Lin, C., Greenwald, D., and Banin, A.: Temperature dependence of infiltration rate during large
583 scale water recharge into soils, Soil Sci. Soc. Am. J., 67, 487–493,
584 https://doi.org/10.2136/sssaj2003.4870, 2003.

585 Mächler, L., Peter, S., Brennwald, M. S., and Kipfer, R.: Excess air formation as a mechanism
586 for delivering oxygen to groundwater, Water Resour. Res., 49, 6847–6856,
587 https://doi.org/10.1002/wrcr.20547, 2013.

588 Massmann, G., Greskowiak, J., Dünnbier, U., Zuehlke, S., Knappe, A., and Pekdeger, A.: The
589 impact of variable temperatures on the redox conditions and the behaviour of pharmaceutical
590 residues during artificial recharge, J. Hydrol., 328, 141–156,
591 https://doi.org/10.1016/j.jhydrol.2005.12.009, 2006.

https://doi.org/10.5194/hess-2021-455
Preprint. Discussion started: 7 October 2021


Hydrology and Earth System Sciences
Discussions

592 McMahon, P. B. and Chapelle, F. H.: Redox processes and water quality of selected principal
593 aquifer systems, Ground Water, 46, 259–271, https://doi.org/10.1111/j.1745-6584.2007.00385.x,
594 2008.

595 Miller, J. H., Ela, W. P., Lansey, K. E., Chipello, P. L., and Arnold, R. G.: Nitrogen
596 Transformations during Soil–Aquifer Treatment of Wastewater Effluent—Oxygen Effects in
597 Field Studies, J. Environ. Eng., 132, 1298–1306, https://doi.org/10.1061/(asce)0733-
598 9372(2006)132:10(1298), 2006.

599 Mizrahi, G., Furman, A., and Weisbrod, N.: Infiltration under Confined Air Conditions: Impact
600 of Inclined Soil Surface, Vadose Zo. J., 15, vzj2016.04.0034,
601 https://doi.org/10.2136/vzj2016.04.0034, 2016.

602 Morrison, C. M., Betancourt, W. Q., Quintanar, D. R., Lopez, G. U., Pepper, I. L., and Gerba, C.
603 P.: Potential indicators of virus transport and removal during soil aquifer treatment of treated
604 wastewater effluent, Water Res., 177, 115812, https://doi.org/10.1016/j.watres.2020.115812,
605 2020.

606 Ben Moshe, S., Weisbrod, N., Barquero, F., Sallwey, J., Orgad, O., and Furman, A.: On the role
607 of operational dynamics in biogeochemical efficiency of a soil aquifer treatment system, Hydrol.
608 Earth Syst. Sci., 24, 417–426, https://doi.org/10.5194/hess-24-417-2020, 2020.

609 Ben Moshe, S., Weisbrod, N., and Furman, A.: Optimization of soil aquifer treatment (SAT)
610 operation using a reactive transport model, Vadose Zo. J., 1–13,
611 https://doi.org/10.1002/vzj2.20095, 2021.

612 Nadav, I., Arye, G., Tarchitzky, J., and Chen, Y.: Enhanced infiltration regime for treated-
613 wastewater purification in soil aquifer treatment (SAT), J. Hydrol., 420–421, 275–283,
614 https://doi.org/10.1016/j.jhydrol.2011.12.013, 2012a.

615 Nadav, I., Tarchitzky, J., and Chen, Y.: Soil cultivation for enhanced wastewater infiltration in
616 soil aquifer treatment (SAT), J. Hydrol., 470–471, 75–81,
617 https://doi.org/10.1016/j.jhydrol.2012.08.013, 2012b.

618 Negev, I., Shechter, T., Shtrasler, L., Rozenbach, H., and Livne, A.: The effect of soil tillage
619 equipment on the recharge capacity of infiltration ponds, 12, 1–11,

https://doi.org/10.5194/hess-2021-455
Preprint. Discussion started: 7 October 2021

620 https://doi.org/10.3390/w12020541, 2020.

621 Nimmo, J. R., Schmidt, K. M., Perkins, K. S., and Stock, J. D.: Rapid Measurement of Field-
622 Saturated Hydraulic Conductivity for Areal Characterization, Vadose Zo. J., 8, 142–149,
623 https://doi.org/10.2136/vzj2007.0159, 2009.

624 Oren, O., Gavrieli, I., Burg, A., Guttman, J., and Lazar, B.: Manganese mobilization and
625 enrichment during soil aquifer treatment (SAT) of effluents, the Dan Region Sewage
626 Reclamation Project (Shafdan), Israel, Environ. Sci. Technol., 41, 766–772,
627 https://doi.org/10.1021/es060576+, 2007.

628 Quanrud, D. M., Arnold, R. G., Wilson, L. G., Gordon, H. J., Graham, D. W., and Amy, G. L.:
629 Fate of Organics during Column Studies of Soil Aquifer Treatment, J. Environ. Eng., 122, 314–
630 321, https://doi.org/10.1061/(asce)0733-9372(1996)122:4(314), 1996.

631 Quanrud, D. M., Hafer, J., Karpiscak, M. M., Zhang, J., Lansey, K. E., and Arnold, R. G.: Fate
632 of organics during soil-aquifer treatment: Sustainability of removals in the field, Water Res., 37,
633 3401–3411, https://doi.org/10.1016/S0043-1354(02)00489-X, 2003.

634 Reedy, K. R., D'Angelo, E. M., and Harris, W. G.: Biochemistry of wetlands, in: Handbook of
635 Soil Science, edited by: Summer, M. E., 89–119, 2000.

636 Rezanezhad, F., Couture, R. M., Kovac, R., O'Connell, D., and Van Cappellen, P.: Water table
637 fluctuations and soil biogeochemistry: An experimental approach using an automated soil
638 column system, J. Hydrol., 509, 245–256, https://doi.org/10.1016/j.jhydrol.2013.11.036, 2014.

639 Ritter, A. and Muñoz-Carpena, R.: Performance evaluation of hydrological models: Statistical
640 significance for reducing subjectivity in goodness-of-fit assessments, J. Hydrol., 480, 33–45,
641 https://doi.org/10.1016/j.jhydrol.2012.12.004, 2013.

642 Rodríguez-Escales, P., Barba, C., Sanchez-Vila, X., Jacques, D., and Folch, A.: Coupling Flow,
643 Heat, and Reactive Transport Modeling to Reproduce in Situ Redox Potential Evolution:
644 Application to an Infiltration Pond, Environ. Sci. Technol., 54, 12092–12101,
645 https://doi.org/10.1021/acs.est.0c03056, 2020.

646 Sallwey, J., Jurado, A., Barquero, F., and Fahl, J.: Enhanced removal of contaminants of
647 emerging concern through hydraulic adjustments in soil aquifer treatment, 12,

https://doi.org/10.3390/w12092627, 2020.

Sattar, A. M. A.: Prediction of Organic Micropollutant Removal in Soil Aquifer Treatment System Using GEP, J. Hydrol. Eng., 21, 04016027, https://doi.org/10.1061/(asce)he.1943-5584.0001372, 2016.

Schmidt, C. M., Fisher, A. T., Racz, A. J., Lockwood, B. S., and Huertos, M. L.: Linking denitrification and infiltration rates during managed groundwater recharge, Environ. Sci. Technol., 45, 9634–9640, https://doi.org/10.1021/es2023626, 2011.

Sharma, S. K. and Kennedy, M. D.: Soil aquifer treatment for wastewater treatment and reuse, Int. Biodeterior. Biodegrad., 119, 671–677, https://doi.org/10.1016/j.ibiod.2016.09.013, 2017.

Shenker, M., Seitelbach, S., Brand, S., Haim, A., and Litaor, M. I.: Redox reactions and phosphorus release in re-flooded soils of an altered wetland, Eur. J. Soil Sci., 56, 515–525, https://doi.org/10.1111/j.1365-2389.2004.00692.x, 2005.

Silver, M., Knöller, K., Schlögl, J., Kübeck, C., and Schüth, C.: Nitrogen cycling and origin of ammonium during infiltration of treated wastewater for managed aquifer recharge, Appl. Geochemistry, 97, 71–80, https://doi.org/10.1016/j.apgeochem.2018.08.003, 2018.

Skopp, J., Jawson, M. D., and Doran, J. W.: Steady-State Aerobic Microbial Activity as a Function of Soil Water Content, Soil Sci. Soc. Am. J., 54, 1619–1625, https://doi.org/10.2136/sssaj1990.03615995005400060018x, 1990.

Sopilniak, A., Elkayam, R., and Lev, O.: Nitrification in a soil-aquifer treatment system: Comparison of potential nitrification and concentration profiles in the vadose zone, Environ. Sci. Process. Impacts, 19, 1571–1582, https://doi.org/10.1039/c7em00402h, 2017.

Stumm, W., & Morgan, J. J.: Aquatic chemistry (3rd ed.), Wiley, 1996.

Tsangaratos, P., Kallioras, A., Pizpikis, T., Vasileiou, E., Ilia, I., and Pliakas, F.: Multi-criteria Decision Support System (DSS) for optimal locations of Soil Aquifer Treatment (SAT) facilities, Sci. Total Environ., 603–604, 472–486, https://doi.org/10.1016/j.scitotenv.2017.05.238, 2017.

Tufenkji, N., Redman, J. A., and Elimelech, M.: Interpreting deposition patterns of microbial particles in laboratory-scale column experiments, Environ. Sci. Technol., 37, 616–623,

https://doi.org/10.5194/hess-2021-455
Preprint. Discussion started: 7 October 2021

Hydrology and Earth System Sciences
Discussions

675 https://doi.org/10.1021/es025871i, 2003.

676 Wallace, C. D., Sawyer, A. H., and Barnes, R. T.: Spectral analysis of continuous redox data
677 reveals geochemical dynamics near the stream–aquifer interface, Hydrol. Process., 33, 405–413,
678 https://doi.org/10.1002/hyp.13335, 2019.

679

680

681

682

683